

## **General Disclaimer**

### **One or more of the Following Statements may affect this Document**

- This document has been reproduced from the best copy furnished by the organizational source. It is being released in the interest of making available as much information as possible.
- This document may contain data, which exceeds the sheet parameters. It was furnished in this condition by the organizational source and is the best copy available.
- This document may contain tone-on-tone or color graphs, charts and/or pictures, which have been reproduced in black and white.
- This document is paginated as submitted by the original source.
- Portions of this document are not fully legible due to the historical nature of some of the material. However, it is the best reproduction available from the original submission.

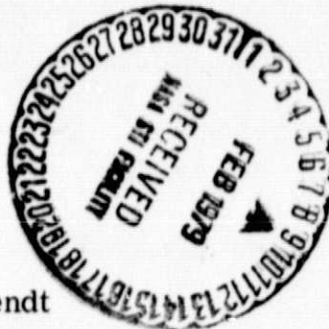
NASA Technical Memorandum 79065

{NASA-TM-79065} SOME PROPERTIES OF AN  
ADVANCED BORON FIBER (NASA) 11 p HC A02/MF  
A01 CSCL 11D

N79-16076

G3/24 Unclass  
43367

SOME PROPERTIES OF AN ADVANCED  
BORON FIBER



Donald R. Behrendt  
Lewis Research Center  
Cleveland, Ohio

TECHNICAL PAPER to be presented at the  
Meeting of the American Ceramic Society  
Merritt Island, Florida, January 22-24, 1979

## SOME PROPERTIES OF AN ADVANCED BORON FIBER

by Donald R. Behrendt

National Aeronautics and Space Administration  
Lewis Research Center  
Cleveland, Ohio 44135

### ABSTRACT

An advanced coreless boron fiber has exhibited tensile strengths which are more than twice that of the normal CVD B/W fibers. The coreless fiber is made by the chemical removal of the tungsten boride core exposed by splitting the as-grown fiber. The easily splittable fiber is made by the chemical vapor deposition of boron on a larger than usual tungsten substrate. It is expected that the ease of splitting is related to residual stresses in these fibers. Measurements of the axial residual stresses in both the normal and the splittable fibers are presented and the results compared. Differences in these stresses are discussed in connection with the ease of splitting in the splittable fibers.

### INTRODUCTION

An advanced boron fiber has been developed for NASA under a contract with the Avco Specialty Materials Division. This new fiber is in many ways very different from the usual boron on tungsten (B/W) fibers presently manufactured. Typically, boron fibers are produced by the chemical vapor deposition (CVD) of boron on a  $12.7\text{ }\mu\text{m}$  (0.5 mil) diameter tungsten-wire substrate from a mixture of gases of boron trichloride and hydrogen. These fibers are usually produced with a final diameter of 102, 142, or  $203\text{ }\mu\text{m}$  (4.0, 5.6, or 8.0 mils) and have a core approximately  $16.3\text{ }\mu\text{m}$  (0.64 mils) in diameter consisting of at least two tungsten borides. Their tensile strengths average from 3450 to  $4140\text{ MN/m}^2$  (500 to 600 ksi). It is known that the strength of CVD boron fibers is limited to these values by cracks which predominantly start either in the tungsten boride core or in the boron near the core.

The advanced boron fiber differs from the usual CVD fiber in that it has no tungsten boride core. This eliminates the core-initiated cracks, resulting in a fiber of considerably increased strength. The method developed to produce this coreless fiber involves the chemical removal of the core of a CVD B/W fiber specially prepared to split easily and expose the core. The easily splittable fiber is produced by depositing the boron on a larger  $25.4\text{ }\mu\text{m}$  (1.0 mil) diameter tungsten substrate using deposition conditions optimized

to produce maximum splittability. The fiber splits into three approximately equal pieces. Hot nitric acid is used to remove the tungsten boride core. Figure 1 is a reproduction of a scanning electron microscope (SEM) micrograph showing a typical split and etched fiber.

As the fibers split they curve slightly in the shape of a stretched-out helix. A way to describe this is that the final fiber has the same shape as one would get by wrapping a small wire around a 2.5 mm (100 mil) diameter rod with each wrap advancing about 25 mm (1.0 in.) along the rod. Figure 2 illustrates this.

Tests made at Avco on these split and etched fibers have shown them to be much stronger than the usual boron fibers. These results are shown in Table I. The average tensile strength of eight pulls was  $7.90 \text{ GN/m}^2$  (1145 ksi) with one pull in excess of  $14 \text{ GN/m}^2$  (2000 ksi). The average strength is about twice that of boron fibers containing a core.

A key factor which makes this method possible is the ease of splitting of as-grown fibers. The ease of splitting is determined by the residual stresses which are known to exist in CVD boron fibers (ref. 1). It is likely that the tensile-circumferential stress in the splittable fiber is larger or extends nearer to the surface than it does in the usual boron fiber. Although we cannot measure directly this component of the residual stress, we can measure the axial component. A method will be described for measuring the axial residual stresses in normal and splittable boron fibers, and the resulting stress distributions for the two types of fibers will be compared.

## EXPERIMENTAL

A dilatometer was designed so that as the surface of the fiber under test was removed by electropolishing, continuous measurements could be made of length changes of the boron-fiber specimen. From these axial strains, the axial residual stress distribution could be calculated. Figure 3 is a schematic representation of the dilatometer. The specimen is mounted between an inner and an outer quartz tube. The inner tube is free to slide vertically in teflon bushings within the outer tube. The boron fiber to be tested is cemented with conducting epoxy between the bottom of the outer tube and a sleeve connected to the inner tube. Normally, the fiber test section is about 1 cm (0.4 in.) long. The center plate of a three-plate capacitor is attached to the top of the inner tube. The outer two plates are insulated from each other and attached to the top of the outer tube. Thus any change in length of the specimen produces an equal change in the position of the center plate with respect to the outer plates. The relative position of the center plate is detected by applying a 100 V, peak-



to-peak 3000 Hz voltage to the outer plates. The resulting signal from the center plate is applied to a high-impedance ( $10\text{ m}\Omega$ ) input of a lock-in amplifier. A strip chart recorder provides a continuous recording versus time of the output of the lock-in amplifier. Calibration showed that the position of the recorder pen was linearly related to the position of the center plate of the dilatometer.

During the measurement, the surface of the boron is removed by electropolishing at room temperature by placing the lower portion of the dilatometer in a low-conductivity solution made by dissolving 0.5 g of sodium hydroxide in  $30\text{ cm}^3$  of water and adding  $150\text{ cm}^3$  of glycerin.

In preliminary tests, it was established that the rate of mass removed from the fiber was constant for a given current independent of fiber diameter. Because the mass-removal rate is constant, the fiber diameter could be calculated within an accuracy of three percent for any time during the run by knowing the final diameter and the time since the start of electropolishing. This allowed the dilatometer to remain undisturbed during an actual run since it was not necessary to make physical diameter measurements of the fiber.

The axial strain,  $\epsilon_z$ , for a time,  $t$ , during electropolishing is calculated from the measurements of fiber length changes. The radius,  $r$ , for the same time,  $t$ , is calculated from the final diameter and total time at the end of electropolishing. For the purposes of calculating the residual stresses, the Young's modulus,  $E$ , and the Poisson's ratio,  $\nu$ , are assumed to be independent of radius. However the values for  $E$  and  $\nu$  for the core material will be different from those of the boron. It is also assumed that the axial strains observed during electropolishing are produced only by axial stresses. This means that we have neglected the effects of nonaxial stresses  $\sigma_r$  and  $\sigma_\theta$  on the axial strain,  $\epsilon_z$ . It is not possible to estimate the error introduced by neglecting these terms as we do not know  $\sigma_r$  and  $\sigma_\theta$  for boron fibers. However,  $\sigma_r$ ,  $\sigma_\theta$ , and  $\sigma_z$  can be calculated from a model (ref. 1) which treats both the boron and core materials as elastic. Removing the surface of the fiber in this model produces axial strains in the fiber which are produced by  $\sigma_r$ ,  $\sigma_\theta$ , and  $\sigma_z$ . If we make the assumption that the axial strains are produced only by axial stresses, we find that the axial stress is overestimated by about 13 percent. In our calculation of the residual stresses, no account was taken of this error.

From the data of axial strain,  $\epsilon_z$  versus the electropolished radius,  $r$ , it is possible to reconstruct the residual stress distribution in the original fiber of initial radius  $r_0$ . The stress  $\sigma(r_0, r)$  at radius,  $r$ , of the original fiber of radius,  $r_0$ , can be related to the axial strain,  $\epsilon_z$ , produced by electropolishing the fiber to a radius,  $r$ , by

$$\sigma(r_o, r) = - \left[ (E_c - E_b) \frac{r_c^2}{r^2} + E_b \right] \cdot \left[ \frac{r}{2} \frac{d\epsilon_z(r)}{dr} + \epsilon_z(r) \right] \quad (1)$$

where

- $E_c$       Young's modulus of the core  
 $E_b$       Young's modulus of the boron  
 $r_c$       radius of the core  
 $r_o$       initial radius of the fiber  
 $r$       distance from center of fiber for which the residual stress is determined  
 $\epsilon_z(r)$     measured axial strain when the fiber is electropolished to a radius  $r$  with  $\epsilon_z(r_o) = 0$

From the experimental results, we are able to compare the residual stress distributions of the unsplit splittable fiber with that of the 102  $\mu\text{m}$  (4.0 mil) diameter normal boron fiber. Because the residual distributions for 102, 142, and 203  $\mu\text{m}$  (4.0, 5.6, and 8.0 mil) diameter B/W fibers are very similar, we are essentially comparing the splittable fiber with all sizes of the normal fiber.

Measurements of the axial strains versus electropolished fiber diameter were made using six samples of each type of fiber, that is, the 119  $\mu\text{m}$  (4.7 mil) diameter splittable fiber and the 102  $\mu\text{m}$  (4.0) diameter normal fiber. The measurements were continued until either the core was reached or the fiber broke. For all the normal 102  $\mu\text{m}$  (4.0 mil) fibers except one, the fibers broke before the core was reached. For the splittable fibers, only one of the six samples tested broke before reaching the core. The larger core of the splittable fiber (32.6  $\mu\text{m}$  (1.3 mils) core diameter for the splittable fiber compared with 16.3  $\mu\text{m}$  (0.64 mils) core diameter for the normal fiber) probably helps in preventing the splittable fibers from breaking during electropolishing.

Using the axial strain versus radius data and the values of 669  $\text{GN/m}^2$  ( $97 \times 10^6$  psi) for the modulus of the core and 393  $\text{GN/m}^2$  ( $57 \times 10^6$  psi) for the boron (ref. 2), the residual stress versus radius was calculated using Eq. (1). The six calculated residual stress distributions for each type of fiber were averaged to produce a single curve for each of the two types of fibers. The variation of any point on an individual curve of a given set from the corresponding point on the average curve was less than  $\pm 15$  percent. The axial residual stresses at a distance  $r$  from the center of the original fiber for the normal and the splittable boron fibers are shown in figure 4. Here we have used the usual convention that positive stresses are tensile and negative stresses are

are compressive. To allow easy comparison between the two curves, the residual stresses are plotted versus the reduced radius,  $r/r_0$ , where  $r_0$  is the radius of the original fiber. Because electropolishing of the fiber was stopped at the core's surface, details of how the residual stress varies in the core could not be determined; although it is possible to determine the core's average stress. These are shown as dashed lines in figure 4.

### DISCUSSION OF RESULTS

Comparing the residual stress distributions for the two types of fibers, we see some general similarities; both types of fibers show compressive stresses at the surface and at the core, and both have a region of tensile stress in the boron near the core. However, in detail, some significant differences can be noted: (1) the difference in slope of the stress versus reduced radius in the region between  $r/r_0$  equal to 0.35 and 0.6, (2) the large difference between the maximum tensile stresses about  $910 \text{ MN/m}^2$  (132 ksi) for the normal fiber and  $590 \text{ MN/m}^2$  (86 ksi) for the splittable fiber, and (3) for reduced radii larger than 0.6, the residual stress for the splittable fiber is algebraically about  $200 \text{ MN/m}^2$  (28 ksi) more positive than that for the normal fiber. The difference between the core stresses  $-1340 \text{ MN/m}^2$  (-194 ksi) for the normal fiber and  $-1220 \text{ MN/m}^2$  (-177 ksi) for the splittable fibers is not considered to be significant since it is not larger than the variation of core stresses seen among the individual values for the splittable fibers.

We now consider how these differences in the residual stresses between the two types of fibers might account for the increased ease of splitting of the splittable fiber. Radial cracks observed in diamond cleaved boron fibers (ref. 3) radiate from the core into the boron. We would expect that such cracks would propagate outward in the region where the circumferential stress is positive and stop near the radius where this stress makes its transition from a tensile to compressive stress. From figure 4, it can be seen that for the normal  $102 \text{ }\mu\text{m}$  (4.0 mil) B/W, the axial stress changes from tensile to compressive at  $r/r_0$  equal to 0.75. This transition is nearly constant for the other sizes of normal B/W. Measurements made on 102, 142, 203, and  $366 \text{ }\mu\text{m}$  (4.0, 5.6, 8.0, and 14.4 mil) B/W fibers show that the transition of the axial residual stress from a tensile to a compressive stress occurs between an  $r/r_0$  of 0.70 to 0.76 (ref. 4). For the splittable fiber, this transition occurs at a larger value of  $r/r_0$  (0.83) than it does for the normal fibers. If this is also true for the circumferential stress, that is, that the transition from tensile to compressive stress of the circumferential stress occurs at a larger value of  $r/r_0$  in the splittable fiber than it does in the normal fiber,

than it would be expected that the radial crack would extend closer to the surface in the splittable fiber. The additional stresses caused by the application of external forces to the fiber during the splitting operation could make it possible to extend the radial crack to the surface in the splittable fiber.

#### REFERENCES

1. D. R. Behrendt, "Longitudinal Residual Stresses in Boron Fibers," NASA TM X-73402, 1976.
2. J. A. DiCarlo, Private Communication.
3. V. J. Krukonis; pp. 517-540 in Boron and Refractory Borides. Edited by V. I. Matkovich. Springer-Verlag, New York, 1977.
4. D. R. Behrendt, "Axial Residual Stresses in Boron Fibers," NASA TM-73894, 1978.



TABLE I. - TENSILE STRENGTH OF  
CORELESS FIBER

Test no.	GN/m <sup>2</sup>	Tensile strength, ksi
1	6.870	996
2	3.925	569
3	3.711	538
4	10.350	1500
5	10.830	1570
6	14.065	2039
7	8.678	1258
8	4.753	689

ORIGINAL PAGE IS  
OF POOR QUALITY

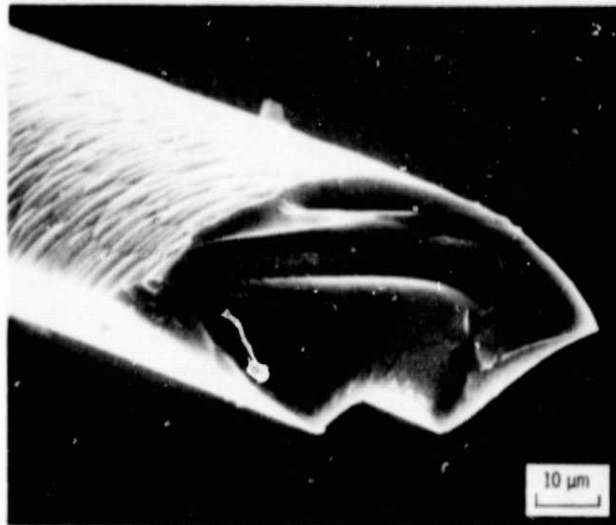


Figure 1. - 4.7 Mil split.

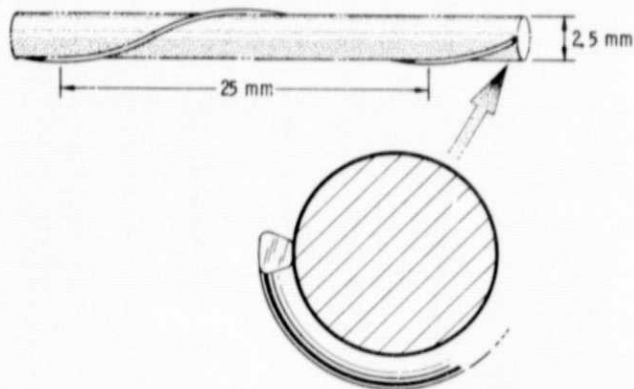


Figure 2. - Illustration of split fiber depicting its curling into a helix. The fiber forms a helix with an amplitude of ~2.5 mm (100 mils) and a period of ~25 mm (1.0 inches).

ORIGINAL PAGE IS  
OF POOR QUALITY

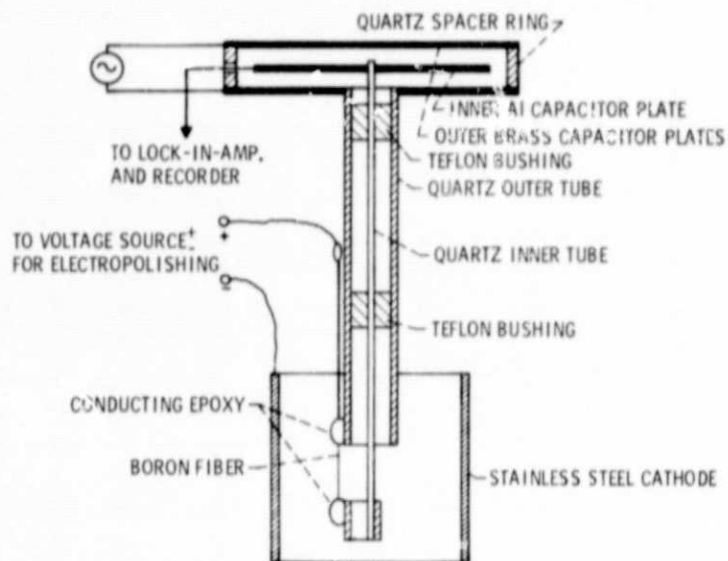


Figure 3. - Dilatometer used to measure length changes of a boron fiber specimen as the fiber's surface was removed by electropolishing.

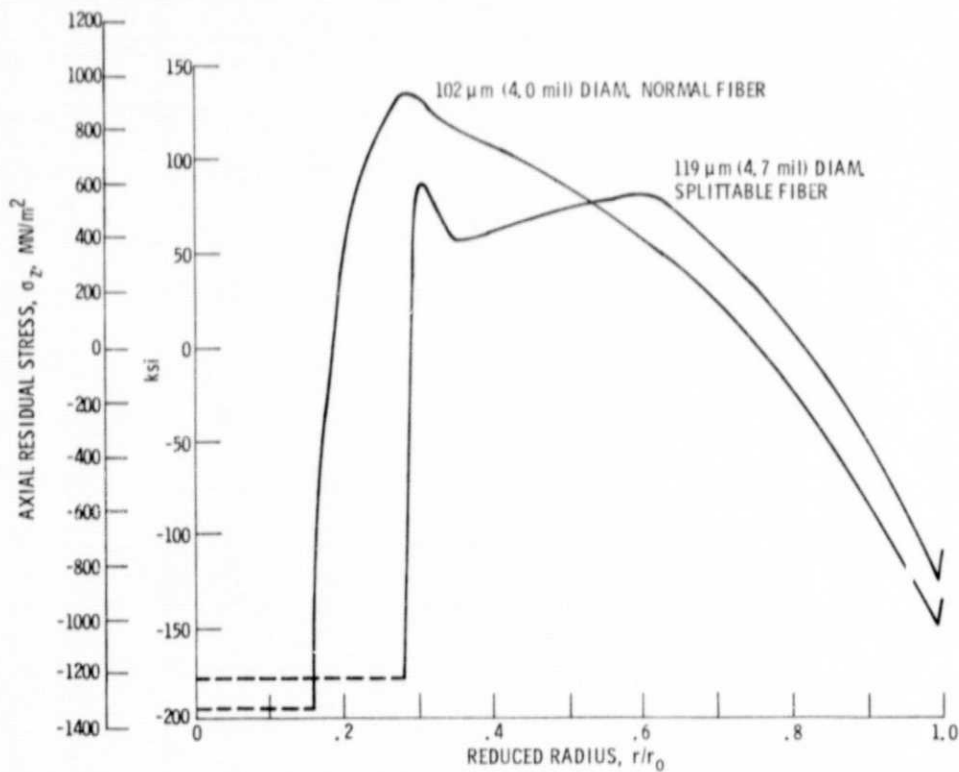


Figure 4. - Plot of the axial residual stress versus reduced radius  $r/r_0$  for the splittable and normal fibers.